Emission and detection of surface acoustic waves by AlGaN/GaN high electron mobility transistors

Lei Shao,[1] Meng Zhang,[2] Animesh Banerjee,[2] Pallab Bhattacharya,[2] and Kevin P. Pipe[1,2,a)]
[1]*Mechanical Engineering, University of Michigan, Ann Arbor, Michigan 48109-2125, USA*
[2]*Electrical Engineering and Computer Science, University of Michigan, Ann Arbor, Michigan 48109-2122, USA*

(Received 16 September 2011; accepted 14 November 2011; published online 15 December 2011)

Using integrated interdigital transducers (IDTs), we demonstrate the emission of surface acoustic waves (SAWs) by AlGaN/GaN high electron mobility transistors (HEMTs) under certain bias conditions through dynamic screening of the HEMTs vertical field by modulation of its two-dimensional electron gas. We show that a strong SAW signal can be detected if the IDT geometry replicates the HEMT electrode geometry at which RF bias is applied. In addition to characterizing SAW emission during both gate-source and drain-source modulation, we demonstrate SAW detection by HEMTs. Integrated HEMT-IDT structures could enable real-time evaluation of epitaxial degradation as well as high-speed, amplified detection of SAWs. © *2011 American Institute of Physics*. [doi:10.1063/1.3665625]

AlGaN/GaN high electron mobility transistors (HEMTs) offer a number of advantages (e.g., wide bandgap, high thermal conductivity) for high-power and high-speed RF and microwave applications.[1] In these applications, material degradation due to thermal[2] and acoustic[3,4] stresses can pose a significant problem, prompting studies of device reliability.[5] Furthermore, GaN-based materials exhibit large acoustic velocities, low acoustic attenuation, and strong piezoelectric effects,[6] leading to their use in gigahertz band surface acoustic wave (SAW) devices.[7–9] For example, studies have shown that the attenuation of SAWs propagating in a AlGaN/GaN heterostructure can be controlled by a DC-biased diode that depletes the two-dimensional electron gas (2DEG) between the interdigital transducer (IDT) emitter/receiver pair.[10] While monolithically integrated HEMTs have been used to amplify the electronic signal output by an IDT[11] and HEMT characteristics have been shown to be affected by flexural modes when the HEMT is grown on an electromechanical resonator,[12] no studies have examined the direct interaction of SAWs and HEMTs, i.e., the generation or detection of SAWs by a 2DEG that is dynamically modulated in the various regimes of transistor operation (e.g., cut-off, linear, and saturation) possible for a 3-terminal HEMT.

SAWs emitted by a HEMT could provide a means to nondestructively sample the degradation of its epitaxy and 2DEG in real time, since SAW attenuation depends strongly on crystal quality.[13] The piezoelectric conversion of emitted SAWs could also provide a means for resonant cooling or energy harvesting in high-power applications. Furthermore, SAWs incident on a HEMT could provide dynamic strain modulation of the HEMT (and thereby modulate carrier concentration[12] and carrier mobility) over short times, potentially without the degradation that often occurs when such strain is incorporated through lattice mismatch. Likewise, HEMT-based SAW detectors could provide direct electrical amplification of SAW signals.

Optical reflectance studies have shown strong generation of coherent acoustic phonons near the drain of a HEMT due to dynamic screening of the 2DEG.[14] Here, we use integrated IDTs to confirm both the generation and detection of SAWs by AlGaN/GaN HEMTs and study the dependence of these mechanisms on HEMT frequency and DC bias conditions.

The integrated HEMT-IDT structure (Fig. 1) was based on an undoped heterojunction consisting of 20 nm AlN, 1 μm GaN, 20 nm $Al_{0.25}Ga_{0.75}N$, and a 2 nm GaN cap grown by molecular beam epitaxy on a sapphire (0001) substrate. The AlGaN/GaN lattice mismatch strain creates a built-in piezoelectric polarization field at the heterointerface, which causes a 2DEG to accumulate.[15] HEMTs were fabricated by chlorine etching mesas and e-beam evaporating Ti/Al/Ti/Au ohmic contacts (subsequently exposed to rapid thermal annealing) and Ni/Au Schottky gates. Processed HEMTs had 1 -μm-wide gates equidistant between 7 -μm-wide source and drain contacts that

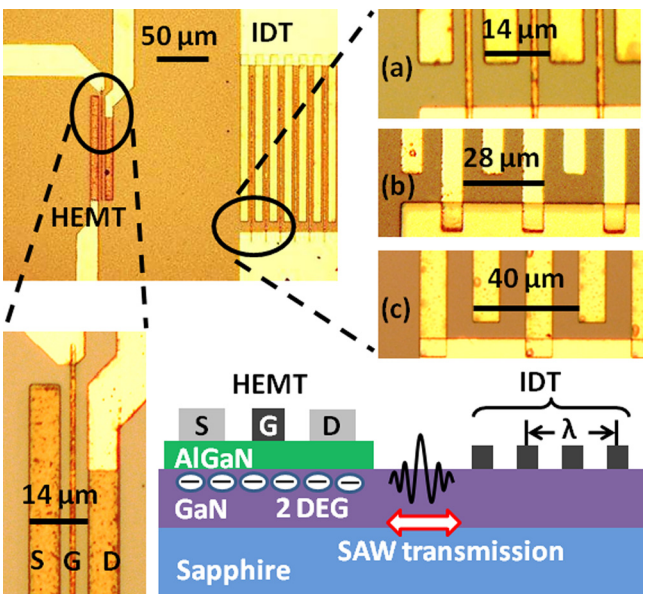

FIG. 1. (Color online) Integrated HEMT-IDT structure, where IDT replicates the gate-source geometry (a), the drain-source geometry (b), or neither (c).

a)Author to whom correspondence should be addressed. Electronic mail: pipe@umich.edu.

 © 2011 American Institute of Physics

had a 7 μm separation. Ni/Au IDTs were formed during gate deposition: one IDT geometry had an electrode periodicity of 14 μm with the same widths and spacing as the HEMT source and gate (Fig. 1(a)), a second had an electrode periodicity of 28 μm with the same widths and spacings as the HEMT source and drain (Fig. 1(b)), and a third had a larger electrode geometry with periodicity 40 μm that was not resonant with the HEMT geometry (Fig. 1(c)). IDT-IDT pairs were also fabricated for each of these geometries to characterize the SAW properties of the epitaxial layers; transmission characteristics were measured for both as-grown (unetched) heterostructures (corresponding to the HEMT layers in which SAWs were generated) and etched heterostructures (corresponding to the region outside of the HEMT through which SAWs propagated). The distances between HEMTs and IDTs and between IDT pairs were nearly the same (approximately 120 μm).

HEMTs and IDTs were contacted by standard microwave probes and operated by a network analyzer, DC power supply, and bias tee. IDT-to-IDT transmission characteristics of the unetched heterostructure (Fig. 2(a)) for the 14 μm IDT geometry (Fig. 1(a)) showed SAW peaks corresponding to the Rayleigh (R) and pseudo-bulk (PB) modes[7] of the epitaxial layer structure. The Rayleigh mode is primarily confined to the thin film epitaxy, while the pseudo-bulk mode is primarily confined to the sapphire substrate near its interface with GaN.[9] IDT-IDT transmission characteristics of the etched heterostructure (Fig. 2(a)) showed significantly lower insertion loss due to the removal of the 2DEG and consequent reduced attenuation;[16] however, the etching process introduces surface roughness which is expected to contribute to SAW scattering. Impedance mismatch in IDT-IDT and HEMT-IDT structures as well as mass loading by the thick electrodes[16] also contribute to insertion loss.

When the drain-source voltage (V_{DS}) of the HEMT was held at 10 V and the gate-source voltage (V_{GS}) was driven

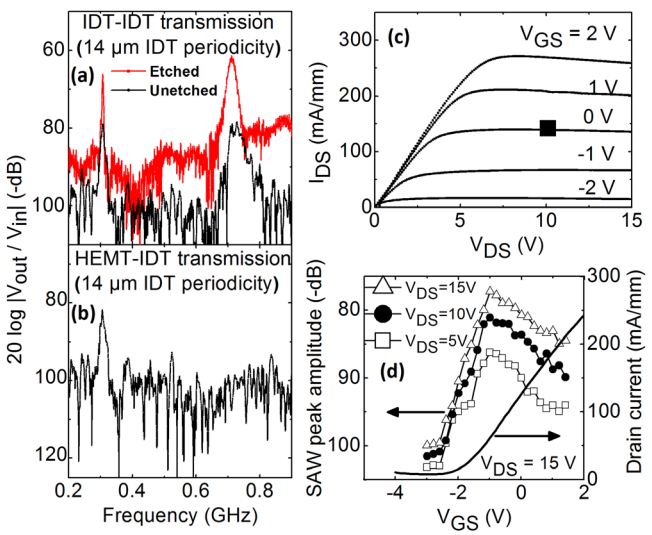

FIG. 2. (Color online)(a) IDT-IDT transmission for unetched (etched) samples showing SAW peaks at 307.7 (306.5) and 713.2 (712.0) MHz corresponding to the Rayleigh and pseudo-bulk modes of the epitaxial layer structure, respectively. IDT geometry is that of Fig. 1(a). (b) HEMT-IDT transmission with $V_{DS} = 10$ and $V_{GS} = 0 + 1.8V_{P\text{-}P}$ showing SAW peak at 307.7 MHz corresponding to the Rayleigh mode in (a). (c) HEMT DC characteristics and bias point in (b). (d) Amplitude of (b) SAW peak as a function of V_{DS} and the DC component of V_{GS}.

with a 1.8 V peak-to-peak ($V_{P\text{-}P}$) RF signal about 0 V, a 307.7 MHz peak was detected at the IDT in the gate-source geometry (Fig. 1(a)) as shown in Fig. 2(b). This peak frequency was the same as that of the Rayleigh mode in the IDT-to-IDT geometry, confirming the emission of SAWs by the modulated HEMT. The larger insertion loss of the HEMT-IDT structures compared to that of the etched IDT-IDT structures is likely primarily due to the much smaller number of "fingers" in the HEMT (1 pair) than in the transmitter IDT (30 pairs).

The amplitude of the 307.7 MHz SAW peak is plotted versus $V_{GS,DC}$ for several V_{DS} values in Fig. 2(d). The drain current (I_{DS}) indicates a HEMT threshold voltage (V_{th}) of $V_{GS,DC} = -2$ V. Because the horizontal electric field in the HEMT does not produce strain to first order,[17] we expect the modulation of the vertical electric field (E_Z) across the AlGaN/GaN layers to play the primary role in SAW generation. For all values of V_{DS}, the maximum HEMT-to-IDT SAW transmission occurs when $V_{GS,DC} \approx V_{th} + V_{P\text{-}P}/2 = -1.1$ V; at this bias point, there is a maximum time variation of the carrier density in the 2DEG, to which we ascribe increased SAW generation through the screening of E_Z.[14] Such screening has been predicted through self-consistent Schrödinger-Poisson calculations to be quite significant[18] and has been identified as a mechanism by which stress-induced defects are produced in the AlGaN barrier layer and device degradation occurs.[3] The fact that the pseudo-bulk mode was not observed is further evidence that SAW generation takes place close to the surface (i.e., near the 2DEG) when gate-source modulation (which oscillates the 2DEG carrier density) is applied. Furthermore, Fig. 2(d) shows that the amplitude of the emitted SAW peak increases with higher V_{DS}. We attribute this to increased depletion of carriers in the GaN layer between the gate and drain, leading to greater penetration of the dynamically screened vertical field into the GaN layer and larger spatially averaged vertical field magnitude in this region.[4,19,20]

The fabricated HEMTs were also operated in common-gate mode with V_{GS} held constant and V_{DS} driven with a $1.8V_{P\text{-}P}$ RF signal about a DC bias point. As illustrated in Fig. 3(b), the 28 μm (Fig. 1(b)) IDT geometry detected SAW peaks emitted by the HEMT at Rayleigh and pseudo-bulk frequencies. The fact that both peaks were detected is consistent with the HEMT source and drain acting as conventional IDT fingers when modulation is applied to them, with dynamic strain extending into the substrate. As shown in Figs. 3(c) and 3(d), the magnitudes of these modes are controlled by V_{GS} and maximized for small DC values of V_{DS} and high values of V_{GS}. When V_{GS} is below threshold, the 2DEG is depleted, and the vertical field profile does not change significantly as V_{DS} is varied;[20] hence, the modulation of V_{DS} for low V_{GS} does not lead to significant SAW generation. Above threshold, for small DC values of V_{DS}, dE_Z/dV_{DS} is large (due to carrier depletion effects[4] as discussed above), leading to significant SAW generation as V_{DS} is modulated. As the DC value of V_{DS} increases, dE_Z/dV_{DS} saturates,[20] leading to reduced SAW generation. In addition to this effect, it is well known that SAW generation is not as strong when Ohmic contact fingers are formed on a conductive substrate,[8] which is the case for the HEMT's source and drain electrodes. This was confirmed by separate

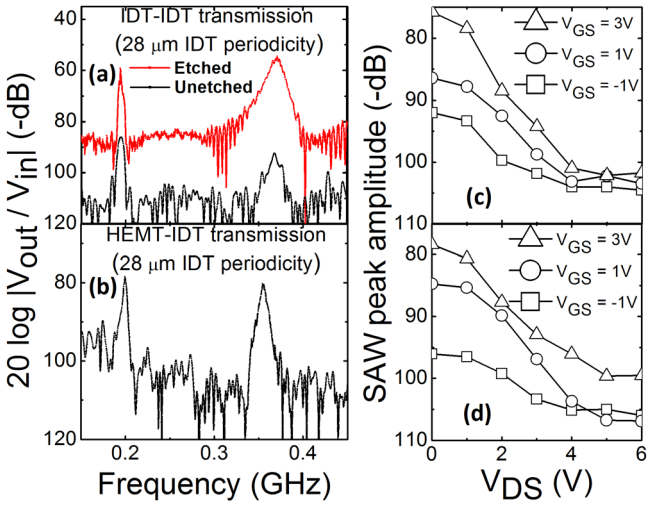

FIG. 3. (Color online) (a) IDT-IDT transmission for unetched (etched) samples showing SAW peaks at 194.8 (194.2) and 368.4 (370.8) MHz corresponding to the Rayleigh and pseudo-bulk modes, respectively. IDT geometry is that of Fig. 1(b). (b) HEMT-IDT transmission with $V_{GS} = 3$ V and $V_{DS} = 1 + 1.8V_{P\text{-}P}$, showing SAW peaks at 195.1 and 368.4 MHz. Amplitudes of the (c) 195.1 MHz and (d) 368.4 MHz SAW peaks from (b) are shown as a function of the DC component of V_{DS}.

measurements we made using IDT-IDT pairs in which all fingers were ohmic, which showed that SAW generation became weaker as the DC bias point about which the RF signal was added increased.

Finally, an IDT with a periodicity of 40 μm (Fig. 1(c)) was used to transmit SAWs to a HEMT with both V_{GS} and V_{DS} held at a constant DC bias point. The AC admittance ($I_{DS,AC}/V_{IDT,AC}$) was used to quantify the detection of the SAW by the HEMT and is plotted in Fig. 4(b). The Rayleigh mode is clearly visible in the AC admittance spectrum, demonstrating that the HEMT can sensitively detect piezoelectric modulation of the 2DEG that occurs when a Rayleigh mode (confined at the surface) passes through it. As shown in Fig. 4(d), the AC admittance amplitude is controlled by V_{GS} and roughly follows the HEMT DC characteristics shown in Fig. 4(c). When the HEMT is biased in its linear regime, the 2DEG density is relatively uniform from the source to the drain, so the small carrier density variation caused by the strain modulation has negligible effect. When the HEMT enters its saturation regime, however, pinch-off of the 2DEG occurs on the drain side; even a small variation of the carrier density in the pinch-off region caused by the strain wave has a significant effect on the HEMTs electrical characteristics, causing the AC admittance to rise rapidly. This change in admittance can be greatly increased by impedance-matching the RF source and IDT, which is expected to increase the magnitude of the generated SAW mode by as much as a factor of 1000.[8]

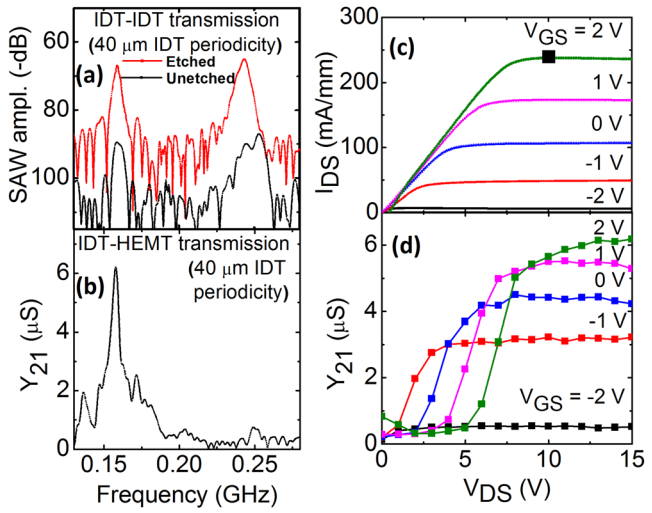

FIG. 4. (Color online) (a) IDT-IDT transmission for unetched (etched) samples showing SAW peaks at 158.8 (158.6) and 253.3 (243.2) MHz corresponding to the Rayleigh and pseudo-bulk modes, respectively. IDT geometry is that of Fig. 1(c). (b) IDT-HEMT transmission with $V_{GS} = 2$ V and $V_{DS} = 10$ V showing admittance peak at 158.8 MHz corresponding to the Rayleigh mode in (a). (c) HEMT DC characteristics and bias point. (d) Amplitude of the 158.8 MHz peak from (b) as a function of V_{DS}. The HEMT detects the SAW when it is biased in the saturation region.

This work was supported by the Defense Advanced Research Projects Agency's Young Faculty Award program under Grant No. N66001-09-1-2106.

[1]L. F. Eastman, V. Tilak, J. Smart, B. M. Green, E. M. Chumbes, R. Dimitrov, H. Kim, O. S. Ambacher, N. Weimann, T. Prunty *et al.*, IEEE Trans. Electron Devices **48**, 479 (2001).
[2]T. Battern, J. W. Pomeroy, M. J. Uren, T. Martin, and M. Kuball, J. Appl. Phys. **106**, 094509 (2009).
[3]J. A. del Alamo and J. Joh, Microelectron. Reliab. **49**, 1200 (2009).
[4]A. Sarua, H. Ji, M. Kuball, M. J. Uren, T. Martin, K. J. Nash, K. P. Hilton, and R. S. Balmer, Appl. Phys. Lett. **88**, 103502 (2006).
[5]G. Meneghesso, G. Verzellesi, F. Danesin, F. Rampazzo, F. Zanon, A. Tazzoli, M. Meneghini, and E. Zanoni, IEEE Trans. Device Mater. Reliab. **8**, 332 (2008).
[6]F. Bernardini, V. Fiorentini, and D. Vanderbilt, Phys. Rev. B **56**, R10024 (1997).
[7]J. Pedrós, F. Calle, J. Grajal, R. J. Jiménez Riobóo, Y. Takagaki, K. H. Ploog, and Z. Bougrioua, Phys. Rev. B **72**, 075306 (2005).
[8]S. H. Lee, H. H. Jeong, S. B. Bae, H. C. Choi, J. H. Lee, and Y. H. Lee, IEEE Trans. Electron Devices **48**, 524 (2001).
[9]F. Calle, J. Pedrós, T. Palacios, and J. Crajal, Phys. Status Solidi C **2**, 976 (2005).
[10]J. Grajal, F. Calle, J. Pedrós, and T. Palacios, IEEE MTT-S Int. Microwave Symp. Dig. **1**, 387 (2004).
[11]K. Y. Wang, W. C. W. Tang, K. M. Lau, and K. J. Chen, in *Proceedings of the Ultrasonics Symposium,* Vancouver, Canada, 2-6 October (IEEE, New York, 2006), p. 281.
[12]M. Faucher, B. Grimbert, Y. Cordier, N. Baron, A. Wilk, H. Lahreche, P. Bove, M. François, P. Tilmant, T. Gehin *et al.*, Appl. Phys. Lett. **94**, 233506 (2009).
[13]D. Schneider and M. D. Tucker, Thin Solid Films **290–291**, 305 (1996).
[14]J. H. Song, Q. Zhang, W. Patterson III, A. V. Nurmikko, M. J. Uren, K. P. Hilton, R. S. Balmer, and T. Martin, Appl. Phys. Lett. **83**, 1023 (2003).
[15]O. Ambacher, B. Foutz, J. Smart, J. R. Shealy, N. G. Weimann, K. Chu, M. Murphy, A. J. Sierakowski, W. J. Schaff, L. F. Eastman *et al.*, J. Appl. Phys. **87**, 334 (2000).
[16]J. Pedrós, F. Calle, R. Cuerdo, J. Grajal, and Z. Bougrioua, Appl. Phys. Lett. **96**, 123505 (2010).
[17]I. L. Guy, S. Muensit, and E. M. Goldys, Appl. Phys. Lett. **75**, 4133 (1999).
[18]B. Jogai, J. D. Albrecht, and E. Pan, J. Appl. Phys. **94**, 3984 (2003).
[19]A. Sarua, H. Ji, J. W. Pomeroy, M. J. Uren, T. Martin, and M. Kuball, Semicond. Sci. Technol. **25**, 085004 (2010).
[20]F. Gao, "Degradation study of AlGaN/GaN HEMT through electro-thermo-mechanical calculations and thermo-reflectance measurements," S.M. thesis, Department of Materials Science and Engineering, Massachusetts Institute of Technology, Boston, MA, 2010.